Available online at www.sciencedirect.com

SciVerse ScienceDirect

Procedia CIRP 00 (2017) 000–000

www.elsevier.com/locate/procedia

3rd CIRP Conference on BioManufacturing

Manufacturing Choices for Ankle-Foot Orthoses: A Multi-objective Optimization

Deema Totah[a,*], Ilya Kovalenko[a], Miguel Saez[a], Kira Barton[a]

[a]*Mechanical Engineering Department, University of Michigan, Ann Arbor, MI 48109, U.S.A.*

[*] Corresponding author. Tel.: +1-617-460-9954. *E-mail address:* deema@umich.edu

Abstract

Increased interest in additive manufacturing (AM) of medical devices leads to a greater number of manufacturing choices, from processes to product designs, with little research comparing these new techniques. This paper proposes a multi-objective optimization approach for choosing the appropriate process, material and thickness that minimizes production cost and time, and maximizes device performance. We tested our framework with a simulated case study to choose between traditional plaster casting and two AM techniques for an ankle-foot orthosis. This evaluation tool provides early quantitative support for AM, and it can be expanded to fit various patient, clinic and insurance provider needs.

Peer-review under responsibility of the scientific committee of the 3rd CIRP Conference on BioManufacturing 2017.

Keywords: AFO, Additive Manufacturing, 3-D Printing, SLS, FDM, Optimization

1. Introduction

An ankle-foot orthosis (AFO) is a custom-made medical device used to correct a patient's walking gait. AFOs are prescribed to individuals with various lower-extremity disabilities, ranging from patients with debilitating disorders like cerebral palsy [1], to multiple sclerosis [2] and stroke recovery patients [3], as well as injuries due to sports and recreation [4].

AFOs come in various shapes and sizes with different stiffness values that correspond to varying levels of movement flexibility to accommodate the diverse populations needing assistance. Some designs involve hinged AFOs that allow/restrict various ranges of ankle motion, others do not include a joint and are referred to as non-articulated AFOs. Both articulated and non-articulated designs may offer energy return either through added elastic components or a leaf spring design [5,6]. The traditional and most-widely adopted method for AFO manufacturing involves plaster casting [7], which is a highly-customized patient-centered process. Plaster casting is also an imperfect process producing non-repeatable results and is highly dependent on skilled labor.

More recently, additive manufacturing (AM) methods have been proposed as alternatives to the traditional approach. Several published studies [5,8–10] outline novel AFO manufacturing methods utilizing foot scanning, computer-aided design (CAD) and additive manufacturing. For example, Faustini et al. [9] outline AFO production through selective laser sintering (SLS), while Jin et al. [10] propose a fused deposition modeling (FDM) AM technique. Both AM approaches require scanning of the foot and utilizing AFO model simulations [5,8,11]. AM pioneers claim that these methods will improve production times, lower waste, decrease costs, and improve AFO performance. Additionally, an AM approach has the potential to lead to greater customization, and enhanced repeatability. Despite the multitude of potential benefits, adoption of AM fabrication of AFOs has been very slow. One key reason for this stems from the lack of quantitative and qualitative metrics comparing AM to more standard manufacturing approaches. As AM technologies become more popular, a clinic's ability to identify the optimal manufacturing method for a specific custom device will become increasingly important.

In this paper, we propose a multi-objective optimization approach to compare the different manufacturing methods and associated materials. We present a framework that identifies the optimal combination of process, material and material thickness that balances cost, production time and patient performance for various AFO sizes. The framework is implemented with a simulated clinic case study explained in section 2. The objective of this work was to develop a methodology for augmenting the design process for a clinician. The framework is meant to serve as a guideline and its parameters may be adjusted according to a clinic's available technologies and individual costs as well as to specific patients' performance and anthropometry. This optimization tool could provide a quantitative approach for synthesizing the different design and performance requirements to provide an optimal solution for design.

Peer-review under responsibility of the scientific committee of the 3rd CIRP Conference on BioManufacturing 2017.

Table 1. Manufacturing processes and associated materials and thickness options used in the case study implementation of the optimization framework.

Process	Materials	Thicknesses (inch)
Plaster Casting	Polypropelyne (PP), Polyethelyne (PE)	$\frac{3}{32}, \frac{1}{8}, \frac{3}{16}, \frac{1}{4}$
SLS	Rilsan D80 (RD80), DuraForm PA (DFPA), DuraForm GF (DFGF), PP, PE	0.03 to 1 with resolution 0.01
FDM	Carbon Fiber Reinforced Polymer (CFRP), PP, PE	0.03 to 1 with resolution 0.01

2. Current AFO Manufacturing Technique

The most-widely adopted AFO manufacturing method is plaster casting [7]. After a referral from a physician, a patient will come into the clinic where an orthotist takes relevant anthropometric measurements and fits the patient with a cast mold by wrapping the affected leg in a plaster wrap. Plaster is then poured into the resulting negative mold to produce a positive mold of the leg. The orthosis is then made by heating and vacuum-forming sheets of thermoplastic onto the plaster mold, which is left to cool and then cut to the correct orthosis shape. Polypropelyne (PP) and polyehtylene (PE) are commonly used thermoplastics [7]. Alternatively, a carbon fiber reinforced polymer-based (CFRP) orthosis might be made in a meticulous, manual layering and lamination process. Additional steps might be involved, depending on the patient's needs, where the plaster mold might be modified or additional components added. Accessories and straps are added to finalize the orthosis production and the patient returns for a fitting visit, where further adjustments might be needed. This is a highly customized process and involves one-on-one interaction between the orthotist and the patient, which allows the patient to give verbal feedback regarding the comfort and support of the orthosis. It also allows the orthotist to visually evaluate the AFO's functionality while in use. However, this process lacks quantitative evaluation metrics. Moreover, the process could take from one to several days, sometimes with weeks between patient visits, and might require several return visits depending on the patient's needs. The plaster casting method produces a lot of wasted materials, which can be costly, and it requires skilled labor to complete this highly manual build.

3. Simulated Case Study

The framework proposed in this paper solves an optimization problem from a simulated case study of a clinic faced with choosing between traditional plaster casting and additive manufacturing for producing its AFOs. The clinic must decide on the manufacturing method, material and thickness that would minimize production cost and time and maximize performance for an AFO of a specific size. Three sizes are simulated in this implementation (section 4.1). For simplicity, our implementation considered only a non-articulated AFO with a leaf spring design, however the algorithm is modular and can be expanded to other designs as more data becomes available.

The clinic is assumed to have access to three manufacturing processes: traditional plaster casting, and two additive manufacturing processes, SLS and FDM. Certain materials can be used and certain thicknesses can be produced with each process, as shown in table 1. For instance, the AM processes can print a range of AFO thicknesses with a minimum resolution of 0.01 inch, while the plaster casting process uses sheets of material with discrete thicknesses. For SLS, process and material information was obtained from [9] and production cost and time from [12]. Information from [7,13] and [10] informed the plaster casting and FDM process assumptions, as well as word-of-mouth and internal documents at the University of Michigan Orthotics and Prosthetics Center.

4. Optimization Framework Setup

The following subsections describe the mathematical setup and implementation of this framework for the simulated case study. Due to the custom nature of these devices and the variability of patient anthropometry, a wide range of AFO sizes may be manufactured. Thus, the model takes the size of the AFO as an input, and in this implementation, three AFO sizes were investigated as explained in section 4.1. The weights and geometries associated with each size were determined using published weight [14] and anthropometry data [15]. The model uses the AFO size input to determine size-dependent variables, such as stiffness, through regression functions based on finite element analysis (FEA) results (section 4.2). The design variables used in the mathematical representation of this framework are described in section 4.3. Finally, section 4.4 details the optimization constraints in terms of the design variables.

4.1. Model Input Variable

The optimization algorithms take the size of the AFO as an input. Our implementation allows the user three sizes to choose from: small, medium and large. Each of the sizes is associated with corresponding patient data: weight, foot length, calf circumference and calf height. The patient measurements for the small, medium and large sizes were respectively chosen as the values of the 10^{th}, 50^{th}, and 90^{th} percentiles of population data published in [14] and [15]. A CAD model of a non-articulated AFO was produced and adjusted for each of the three sizes. The foot and calf measurements determined the geometry of the CAD model, on which finite element analysis (FEA) was performed (section 4.2). The patient weight values determined the ankle moment values simulated in the FEA analysis. The FEA results then determined the safety factor constraint (section 4.4) and performance metric (section 5.3).

Table 2. The anthropometric measurements (calf circumference, calf height, and foot length) and patient weight values used for each AFO size taken from the 10^{th}, 50^{th}, and 90^{th} percentiles of published data from [14] and [15].

		Anthropometry (cm)		
Size	Wt. (Kg)	Calf Circ.	Calf Ht.	Ft. Lgth.
Small	53.5	33.4	320	25.1
Medium	70.3	36.4	354	26.7
Large	101.8	40.1	389	28.4

4.2. Finite Element Analysis

Part performance is affected by design factors (material, thickness, and dimensions), and external factors (load from the user). In order to analyze the effect of both design and external factors, we performed FEA using Autodesk® Inventor™ software. We simulated every combination of material, thickness, AFO size and ankle moment, as mentioned in section 4.1.

The focus of this analysis was: 1) to evaluate yield through the safety factor, and 2) to calculate AFO deflection from the torque applied during ankle plantarflexion. The deflection is used to calculate an effective ankle stiffness of a particular design, which is related to device performance (section 5.3).

In order to reduce computational time a simplified geometry was created based on the geometry of a scanned 3D model of an AFO. This reduced the number of nodes in the simulation. The mesh in the model was adjusted to increase density in the critical areas. Also, a 10% convergence requirement was specified to ensure correct results. Figure 1 shows the scanned, simplified and meshed geometry. The load used in the simulation was determined based on ankle torque for patients with disability [17] and converted into $N\,m\,Kg^{-1}$. This value was then multiplied by the appropriate patient weight based on the AFO size (see table 2), to determine the applied torque value for that size. The anthropometric dimensions of calf circumference, foot length and calf height for the 10th, 50th and 90th percentiles, were similarly used to generate three CAD models of the AFO.

Each of the models was subjected to the appropriate torque loading according to their size. The maximum stress and displacement of the AFO at the calf were extracted from the FEA simulations. The equivalent ankle stiffness was calculated from the resulting displacement. The safety factor was calculated as a ratio of the maximum stress and the material strength.

An FE analysis was run for each of the sizes with each material and each of the four discrete thicknesses of the plaster casting process shown in table 1. The safety factor and ankle stiffness was determined from the FEA for each size, material and thickness combination. Moreover, a regression model was implemented to correlate safety factor and stiffness to the entire range of thicknesses with an R^2 between 0.8 and 1.0.

4.3. Model Design Variables

The mathematical model representing this optimization problem includes several design variables: the type of process, p, the material, m, and the thickness of the material, k, used to create the AFO. There are a processes available with b total possible materials.

One vector, x, was created containing $a + b + 1$ variables:

$$x_i \in \{0, 1\}, \text{ for } i = 1, 2, ..., a + b, \text{ and}$$
$$x_{a+b+1} = k, \text{ where}$$
$$k \in \{y \mid 0.03 < y < 1, y = 0.01n, n \in \mathbb{Z}_+\} \cup \{\tfrac{3}{32}, \tfrac{1}{8}, \tfrac{3}{16}, \tfrac{1}{4}\}$$

$x_1, x_2, ..., x_a$ are binary decision variables indicating the selected process; $x_{a+1}, x_{a+2}, ..., x_{a+b}$ are binary decision variables of the material chosen; and x_{a+b+1} is the variable representing the thickness of that material, which includes all the discrete thicknesses of the additive manufacturing processes (in increments of the minimum resolution) and the four discrete thicknesses of the plaster casting method. This implementation involved three processes ($a = 3$) and six materials ($b = 6$).

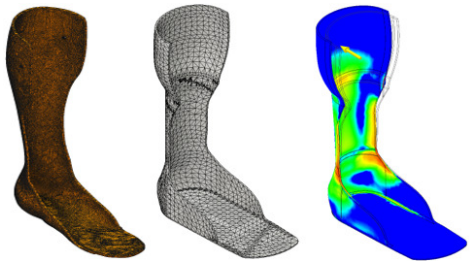

Fig. 1. From left to right, a 3-dimensional scan of a plaster cast AFO, mesh of a modeled AFO, and a contour map showing stresses from an FEA simulation.

4.4. Model Constraints

As mentioned in section 3, there are certain constraints associated with which materials can be selected given the selection of a process for example. The mathematical model representing the optimization problem included several constraints:

1. Only one process can be selected: $(\sum_{j=1}^{a} x_j) - 1 = 0$.
2. Only one material can be selected: $(\sum_{a+1}^{a+b} x_j) - 1 = 0$.
3. If casting is selected, then PP or PE must be selected: $x_1 + (\sum_{j=6}^{9} x_j) - 1 = 0$.
4. If SLS is selected, then PP, PE, RD80, DFPA, or DFGF must be selected: $x_2 + x_4 + x_5 + x_9 - 1 = 0$.
5. If FDM is selected, then PP, PE, or CF must be selected: $x_3 + (\sum_{j=6}^{8} x_j) - 1 = 0$.
6. If casting is selected, then the thickness must be $3/32''$, $1/8''$, $3/16''$, or $1/4''$: $x_1 \prod_{i=1}^{4}(x_{10} - k_i) = 0$, where $k_i = \frac{3}{32}, \frac{1}{8}, \frac{3}{16}, \frac{1}{4}$.
7. The safety factor must be greater than a specified value, SF_{min}, to prevent product yield and failure. The safety factor is a ratio of material strength to maximum stress, calculated as a function of the material chosen, m, the thickness, k, and the AFO size, z: $SF(m, k, z) \geq SF_{min}$. This function was calculated using a combination of FEA and regression analysis (section 4.2).

5. Multi-Objective Optimization

The AFO fabrication analysis is posed as a multi-objective optimization, where a clinic would aim to minimize production cost and time, while maximizing AFO performance.

$$\begin{aligned} &\underset{x}{\text{minimize}} && f_c(x), f_t(x), -f_p(x) \\ &\text{subject to} && \text{contraints } (1) - (7) \end{aligned}$$

The mathematical representation of this objective is a function of the cost, $f_c(x)$, and time, $f_t(x)$, to produce a single AFO, and the performance, $f_p(x)$, of the AFO based on the material, size and thickness chosen. The derivation of each of these functions is described below. The cost and time were determined using data from various literature sources and following a cost analysis method termed 'activity-based costing for manufacturing' outlined in [16]. The performance function was more complex to determine; using published data [17], a performance metric based on predicted patient energetic cost was used.

For our implementation, we resolved the multi-objective optimization into minimizing a single weighted-sum (equation 1). Since production costs are usually carried over to insurance providers, a clinic might value performance and production time more than the cost. The objective weightings chosen followed this logic and were selected empirically after investi-

Table 3. An example of a breakdown for calculating time taken for each process involved in manufacturing an AFO.

Plaster Casting Total Time: 29 hours 11 minutes					
	(1) Impression	(2) Plaster Mold	(3) Adjustment	(4) Shaping	(5) Finishing
Value added time (hr):	1	0.5	1	0.58	0.5
Non-value added time (hr):	0.1	1	0	24.5	0
Number of operators:	1 (Orthotist)	1 (Technician)	1 (Orthotist)	1 (Technician)	1 (Orthotist)
Equipment:	N/A	Miscellaneous	Miscellaneous	Kiln + Vacuum	Miscellaneous
Selective Laser Sintering (SLS) **Total Time: 32 hours 57 minutes**					
	(1) Surface Model	(2) Build CAD	(3) Fabrication	(4) Cleaning	
Value added time (hr):	0.2	0.45	26	0.3	
Non-value added time (hr):	0	0	6	0	
Number of operators:	1 (Orthotist)	1 (Technician)	1 (Technician)	1 (Technician)	
Equipment:	Laser Scanner	PC + Software	SLS Machine	Miscellaneous	
Fused Deposition Modeling (FDM) **Total Time: 26 hours 9 minutes**					
	(1) Surface Model	(2) Build CAD	(3) Fabrication	(4) Finishing	
Value added time (hr):	0.45	0.45	0.1	1.5	
Non-value added time (hr):	0	0	24	0	
Number of operators:	1 (Orthotist)	1 (Technician)	1 (Technician)	1 (Technician)	
Equipment:	Laser Scanner	PC + Software	3-D Printer	Miscellaneous	

gating the solution space.

$$F = 0.01 f_c(x) + f_t(x) - 100 f_p(x) \tag{1}$$

5.1. Cost

Manufacturing cost is calculated as the sum of direct and indirect costs associated with the part [18]. Direct costs include material and labor directly in contact with the part. Indirect costs include machine cost. Overhead costs such as administrative and production overhead are not evaluated at this stage, working under the assumption that all the manufacturing processes are available in the same shop and processes share administrative expenses. The cost model, f_c, with material, labor and equipment cost terms, is shown in equation 2.

$$f_c = C_M + C_L + C_{EQ} \tag{2}$$

$$C_M = \sum_{i=a}^{a+b} c_{m_{i-a}}[(kx_i + 123.34/c_{m_{i-a}})x_1 + \rho_{i-a}(V_{build}(1-\alpha) + V_{bed}\alpha)x_i x_2 + (V_{part} + V_{sup})x_i x_3]$$

$$C_L = \sum_{i=1}^{3}\sum_{h=1}^{2} c_{l_{i,h}} t_{l_{i,h}} x_i \qquad C_{EQ} = \sum_{i=1}^{3}\sum_{e=1}^{n} c_{eq_{i,e}} t_{eq_{i,e}} x_i$$

ρ : material density — c_m : cost of material
α : material waste rate — c_l : cost of labor
V_{part} : volume of part — c_{eq} : cost of equipment
V_{bed} : volume of machine bed — t_l : labor time
V_{sup} : volume of support material — t_{eq} : machine runtime
e : machine $\in \{1, 2, 3, ..., n\}$
h : operator class $\in \{1, 2 \mid 1$: orthotist, 2: technician$\}$

For the casting process, the material is available in specific sheet dimensions and the price is a function of the material and thickness chosen. Because of the discrete set of sizes available, excess material might be wasted and is included in the cost. For the SLS process, a powder block of material of a fixed volume must be used for each production cycle. Only a portion of this material can be recycled and this is reflected in the cost. Finally, for the FDM process, the excess material is in the form of support material needed to support the shape of the AFO while printing. This is a fixed volume of material, $9\,inch^3$ in our case study, with a cost dependent on the material chosen.

5.2. Time

Each manufacturing processes has a specific flow and steps involved in making the part. A value stream mapping was developed for every process to identify time and equipment involved. A simplified version of the map is shown in table 3, where value-added time refers to labor time, while non-value added time involves processes that do not require the presence of an employee, for example cooling time or printing time.

The effect of size on the production time was assumed to be negligible for our purposes. The justification of this choice being that the change in size is small compared to the overall product volume and would not greatly affect the additive manufacturing time. As for the plaster casting process, the orthotist and technician would need to spend the same amount of time on a device regardless of its size.

5.3. Performance

Metabolic rate is a widely used metric for evaluating the performance of wearable medical devices. For this particular device, the patient metabolic rate is most directly affected by the

bending stiffness of the AFO [17,19]. A study varying the bending stiffness of an exoskeleton device, emulating an AFO, worn by healthy subjects while they walked on a treadmill showed a relationship to metabolic rate [17]. Leveraging their research, averaged metabolic rate data they obtained from nine subjects were fit to a quadratic function, resulting in equation 3, where k is the stiffness at the ankle measured in $N\,m\,rad^{-1}$ and r is the predicted metabolic rate at that stiffness with units of $W\,Kg^{-1}$. Since reduced metabolic rate indicates better performance, we aimed to maximize performance, which we defined as the reciprocal of metabolic rate.

$$r = 5e^{-6}k^2 - 0.0019k + 2.9 \quad (3)$$

As explained in section 4.2, FEA was used to create functions which took material, thickness and AFO size as an input and returned the stiffness of the device. This stiffness was then inputted into equation 3 to calculate metabolic rate and thus performance. This allowed us to relate material choice, thickness and AFO size to a performance metric for our objective function. FEA was performed for each of the four discrete thicknesses used by traditional plaster casting manufacturing technique (see table 1). A linear regression model, fit to the FEA results, for each size category was used to calculate bending stiffness for the entire range of thickness values.

5.4. Optimization Algorithms

An exhaustive search of the variable space, implemented using Matlab® software (Mathworks Inc., Natick, MA), was possible in our implementation because of the limited number of variables. In addition to the exhaustive search, the optimization was solved using a heuristic search method (Simulated Annealing) to demonstrate that alternative optimization strategies could be employed for larger data sets. The results from these two methods were compared to determine the impact of alternative optimization methods. Increased data sets could be the result of additional processes, a larger variety of potential materials, or a larger range of allowable thickness, in addition to other parameters. While exhaustive searchers return the most accurate result, these methods are impractical for larger data sets and scenarios in which a faster response is desired. This would be particularly true for clinical use, in which the clinicians would employ this method to aid in the design of the AFO. A faster optimization would allow for more design iterations and a more user friendly design tool.

6. Results and Discussion

Using an exhaustive search, all of the design variable combinations were created and evaluated. The result was a total of 1818 points in the design space. After the model constraints were applied, 686, 736, and 676 points remained as part of the feasible set for small, medium, and large sizes respectively, shown in figure 2. A fair range of performance values were reachable by all processes, while cost and time values differed between processes. PC and FDM were able to minimize the objective function more than SLS could, and this is largely due to the higher cost associated with the SLS process. The optimal process, material, and thickness, resulting in a minimum weighted objective function, were found for each size category and are summarized in table 4.

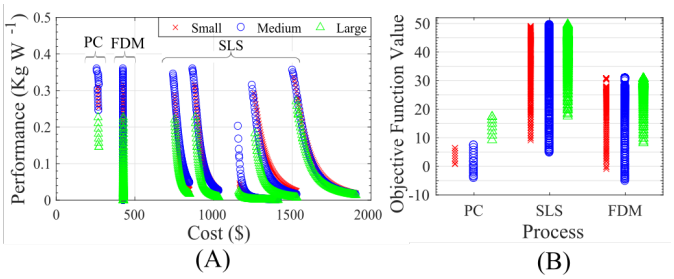

Fig. 2. The (A) cost and performance and (B) objective function value associated with each of the solutions in the feasible set for the three AFO sizes. SLS has the highest cost.

In this case study, FDM was the optimal process. It is the fastest process (see table 3), incurring only a small increase in cost from the plaster casting method, while maintaining comparable performance. It is worth mentioning that machine cycle time is low in SLS, however, SLS machines must warm up before initiation and SLS-manufactured parts require a long cool down time before extraction. Casting is a less expensive process, but it also requires a long cooling time after the plastic has been heat-molded to the plaster. It is worth noting that SLS and FDM both allow batch production. These technologies can leverage economies of scale to produce multiple parts simultaneously, thus shortening setup and production time as well as cost per part. This analysis did not take into account economies of scale as it only considered production of one AFO per batch.

PE and PP were the chosen optimal materials. Upon further investigation, the performance of the PE material was found to be only slightly better (by $0.005\,Kg\,W^{-1}$) than the PP material. PP-PE composites are also sometimes used to manufacture AFOs, however, for simplicity, this case study did not consider this combination. Future work will consider alternative material types. It was also observed that a larger thickness was chosen for the small AFO compared to the medium one. This could be due to the different materials chosen and the change in AFO geometry due to size-specific anthropometric measurements and ankle moment. It seems that the relationship between AFO size and optimal thickness is not a linear one. Further experimental data is required to form a proper stiffness-performance model.

The simulated annealing method was able to find the global optimal solution. However, due to the small number of variables in this problem, simulated annealing proved to be more computationally intensive than the exhaustive search method as shown in table 5. Heuristic methods like simulated annealing are expected to have better performance as the number of variables and options increases. A future implementation that includes a larger variable set could benefit from such a heuristic method. The model could be further expanded to include other

Table 4. The global optimal selections and corresponding optimization function values for each AFO size considered.

	Process	Material	Thickness (in.)	Cost ($)	Time (hr.)	Performance ($Kg\,W^{-1}$)	Obj. Func. Value
Small	FDM	PE	0.17	425.91	26.5	0.35	-3.79
Medium	FDM	PP	0.11	425.90	26.5	0.36	-5.13
Large	FDM	PP	0.19	425.95	26.5	0.23	8.10

Table 5. Comparison of the heuristic simulated annealing (SA) optimization method with an exhaustive search (ES) for the three sizes: small (S), medium (M), and large (L). The success rate was evaluated by running 10 trials of the optimization. The runtime is an average of the runtimes of the 10 trials.

	ES			SA		
Size	S	M	L	S	M	L
Optimal Found?	yes	yes	yes	yes	yes	yes
Success Rate (%)	100	100	100	90	100	100
Runtime (sec.)	2.88	2.84	2.78	4.36	4.99	4.12

sizes, dimensions and AFO designs. It could be adapted to take patient anthropometric measurements as an input instead of a set size (small, medium, and large), build a geometry that fits the patient, and then automatically adjust FEA results accordingly. Such a model would add even more customizability, with potential for creating non-traditional AFO designs. Machine tool paths, AM process parameters and AFO geometries could be optimized simultaneously and scalability could be incorporated, by producing multiple AFOs per batch, to reduce cost and time. The limitation lies in the availability of experimental data to validate FEA results and any resulting models.

This framework provides a quantitative tool for evaluating the optimal choices for these custom devices. For example, it relies on a quantitative model of metabolic rate and stiffness to predict performance. Quantitative models are necessary for insurance reimbursement justification. However, qualitative orthotist input is also necessary. The integration of qualitative feedback can complement the quantitative choices and provide a better full picture. The weights of the multi-objective function could be altered according to the various interests of patient, clinic and insurance provider. With the weights selected in this paper, our quantitative model provides early support for the development of additive manufacturing techniques for AFO manufacturing. However, more complex FEA studies coupled with experimental validation and a better understanding of the properties of additively-manufactured materials is needed. Moreover, a greater understanding of patient performance as various AFO design variables are altered is necessary. With advancements in sensing techniques, the proposed optimization framework could be coupled with real-time sensing methods to more accurately determine an AFO's performance metric.

7. Conclusion

A framework was developed for finding quantitatively optimal manufacturing choices for producing AFO devices. The framework was successfully tested with a simulated case study to show feasibility. A manufacturing process, material and thickness were chosen to optimize cost, time and patient performance for three sizes of an AFO device. As additive manufacturing techniques make their way further into custom-manufactured devices, and as more and more choices become available to patients and clinics, an optimization framework could automate part of the decision process and find a quantitatively optimal solution. This versatile framework provides a guideline for a clinic to evaluate and optimize its choices. However, the framework is limited to available experimental data to inform both patient performance and FEA models.

Acknowledgements

This work was partially supported through NSF PFI Award #1534003, NSF grant #1462910, and a University of Michigan Mechanical Engineering departmental fellowship. The authors thank Darren Bolger, CP, for his feedback and guidance on the plaster casting method, and Robert Chisena for providing a 3-D scan of an AFO.

References

[1] Maltais D, Bar-Or O, Galea V, Pierrynowski M. Use of orthoses lowers the O2 cost of walking in children with spastic cerebral palsy. Medicine and Science in Sports and Exercise. 2001 feb;33(2):320–325.

[2] Sheffler LR, Hennessey MT, Knutson JS, Naples GG, Chae J. Functional effect of an ankle foot orthosis on gait in multiple sclerosis: a pilot study. American journal of physical medicine & rehabilitation / Association of Academic Physiatrists. 2008 jan;87(1):26–32.

[3] Sherk KA, Sherk VD, Anderson MA, Bemben DA, Bemben MG. Lower Limb Neuromuscular Function and Blood Flow Characteristics in AFO-Using Survivors of Stroke. Journal of Geriatric Physical Therapy. 2015;38(2):56–61.

[4] Pommering TL, Kluchurosky L, Hall SL. Ankle and Foot Injuries in Pediatric and Adult Athletes. Primary Care: Clinics in Office Practice. 2005 mar;32(1):133–161.

[5] Mavroidis C, Ranky RG, Sivak ML, Patritti BL, DiPisa J, Caddle A, et al. Patient specific ankle-foot orthoses using rapid prototyping. Journal of neuroengineering and rehabilitation. 2011 jan;8(1):1.

[6] Ounpuu S, Bell KJ, Davis RB, DeLuca Pa. An evaluation of the posterior leaf spring orthosis using joint kinematics and kinetics. Journal of pediatric orthopedics. 1996;16(3):378–84.

[7] International Committee of the Red Cross's Physical Rehabilitation Programme. Manufacturing Guidelines: Ankle Foot Orthosis; 2010.

[8] Lochner SJ, Huissoon JP, Bedi SS. Simulation Methods in the Foot Orthosis Development Process. Computer-Aided Design and Applications. 2014 jun;11(6):608–616.

[9] Faustini MC, Neptune RR, Crawford RH, Stanhope SJ. Manufacture of Passive Dynamic AnkleFoot Orthoses Using Selective Laser Sintering. IEEE Transactions on Biomedical Engineering. 2008 feb;55(2):784–790.

[10] Jin Y, He Y, Shih A. Process Planning for the Fuse Deposition Modeling of Ankle-Foot-Othoses. Procedia CIRP. 2016;42:760–765.

[11] Munguia J, Dalgarno K. Ankle foot orthotics optimization by means of composite reinforcement of free-form structures. In: 24th International SFF Symposium - An Additive Manufacturing Conference, SFF 2013. Austin, Texas, USA; 2013. p. 766–776.

[12] Ruffo M, Tuck C, Hague R. Cost estimation for rapid manufacturing - laser sintering production for low to medium volumes. Proceedings of the Institution of Mechanical Engineers, Part B: Journal of Engineering Manufacture. 2006 jan;220(9):1417–1427.

[13] Chen RK, an Jin Y, Wensman J, Shih A. Additive manufacturing of custom orthoses and prostheses-A review. Additive Manufacturing. 2016;12:77–89.

[14] McDowell MA, Fryar CD, Ogden CL, Flegal KM. Anthropometric reference data for children and adults United States, 2003-2006. National Center for Health Statistics (U.S.); 2008.

[15] White RM. Comparative Anthropometry of the Foot. Army Natick Research and Development Labs (Individual Protection Lab), MA, USA; 1982.

[16] Horngren C, Sundem G, Stratton W, Teall H. Management Accounting. 4th ed. Pearson Canada; 2001.

[17] Collins SH, Wiggin MB, Sawicki GS. Reducing the energy cost of human walking using an unpowered exoskeleton. Nature. 2015 apr;522(7555):212–215.

[18] Dieter GE, Schmidt LC. Engineering design. vol. 3. McGraw-Hill New York; 2013.

[19] Kerkum Y, Harlaar J, van den Noort J, Becher J, Buizer A, Brehm MA. The effects of different degrees of ankle foot orthosis stiffness on gait biomechanics and walking energy cost. Gait & Posture. 2015 sep;42:S89–S90.